J. Phys.: Condens. Matter 6 (1994) A395–A402. Printed in the UK

Formation of two-dimensional colloid crystals in liquid films under the action of capillary forces

P A Kralchevsky†, N D Denkov†, V N Paunov†, O D Velev†, I B Ivanov†, H Yoshimura‡ and K Nagayama‡

† Laboratory of Thermodynamics and Physico-chemical Hydrodynamics, University of Sofia, 1126 Sofia, Bulgaria

‡ Protein Array Project, ERATO, JRDC, 5-9-1 Tokodai, Tsukuba 300-26, Japan

Received 25 October 1993

Abstract. When two similar small particles are attached to a liquid interface they attract each other due to a lateral capillary force. This force appears because the gravitational potential energy of the floating particles decreases when they are approaching each other. This force is proportional to R^6 (R is the particle radius), so it decreases very fast with particle size and becomes negligible for $R < 10$ μm. We found that the situation is quite different when the particles (instead of being freely floating) are partially immersed in a liquid layer on a substrate. In this case the energy of capillary attraction is proportional to R^2 and turns out to be much larger than kT even with particles of diameter about 10 nm. The effect is related to the particle three-phase contact angle, i.e. to the intermolecular forces, rather than to gravity. The experiments show that the lateral capillary forces can bring about the formation of a two-dimensional array (2D-crystal) from both micrometre-size and submicrometre particles: latex spheres, protein globules, etc.

1. Introduction

A fast and convenient method for formation of a two-dimensional (2D) protein array on a mercury surface has been recently developed [1, 2]. The good quality of the samples thus obtained allowed investigation of the protein orientation and structure by electron microscopy combined with image reconstruction. Highly ordered 2D crystals can thus be obtained in a controllable way; this technique could lead to further development of the controlled building up of well ordered protein monolayers and multilayers—a possible step towards a future high technology at the macromolecular level [2]. 2D arrays on solid substrates can find applications in various modern techniques, such as data storage, optical devices and microelectronics [3]. The occurrence of the 2D array formation with proteins [1, 2, 4] in many aspects resembles the ordering process with larger latex particles [5, 6]. It can be expected that the capillary interparticle forces play an important role in both these systems.

The capillary forces between particles attached to an interface have been studied both experimentally [7, 8] and theoretically [9–12]. In the present paper we present a short review of our recent theoretical and experimental studies [13–18] on the different kinds of capillary force. Our aim is to attract the reader's attention to the variety of capillary interactions taking place at two different boundary conditions on the particle surfaces: fixed contact angle and fixed contact line. Particle–wall interactions, giving rise to the so-called 'capillary image forces' are also studied [19, 20].

0953-8984/94/SA0395+08$19.50 © 1994 IOP Publishing Ltd

2. Experiment with latex particles

In our model experiments [5, 6] we investigated the mechanism of 2D array formation using a suspension containing monodisperse particles of 1.70 μm diameter. This was spread over a horizontal hydrophilic glass plate encircled by a Teflon ring. The slightly concave layer formed gradually thins owing to the water evaporation; when its thickness in the centre of the substrate becomes equal to the particle diameter, a nucleus of 2D crystal suddenly forms. The particles in the thicker layer encircling the nucleus begin to move towards the ordered zone and upon reaching the boundary of the array they are trapped in it (figure 1).

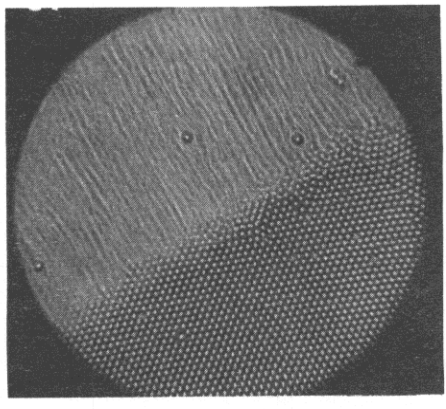

Figure 1. Photograph of the 2D array growth: the tracks of the particles rushing towards the ordered phase are seen.

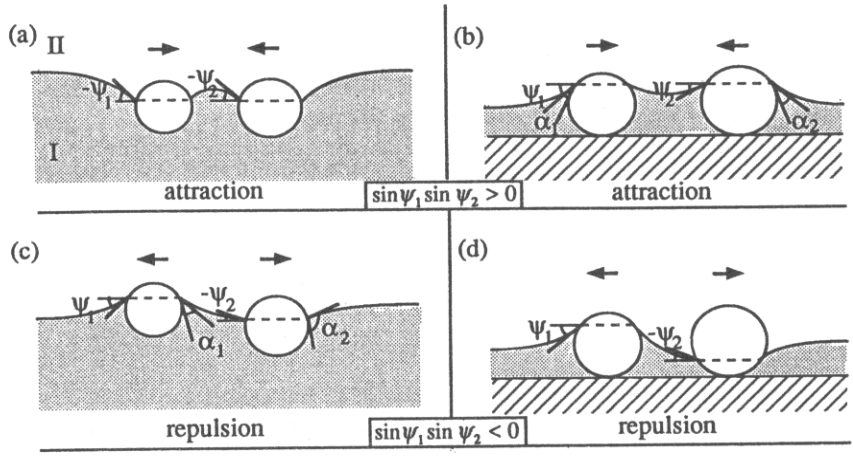

Figure 2. Comparison between the flotation (*a*), (*c*) and immersion (*b*), (*d*) lateral capillary forces; α_k and $\psi_k (k = 1, 2)$ are contact and meniscus slope angles, respectively.

The nature of the forces governing the ordering is revealed by the fact that in all experiments the 2D array formation always began when the thickness of the water layer

became equal to the particle diameter. This implies that the 2D-crystal nuclei are formed under the capillary attraction arising when the tops of the particles protrude from the water layer. The attraction energy can be much larger than the thermal energy (kT) even with nanometer-sized particles [13–16]—see figure 3 below.

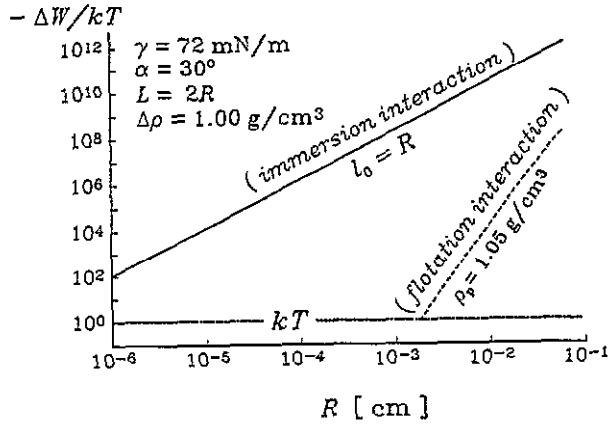

Figure 3. Capillary interaction energy, ΔW, versus particle radius, R, at fixed interparticle distance, $L = 2R$, for immersion and flotation capillary forces.

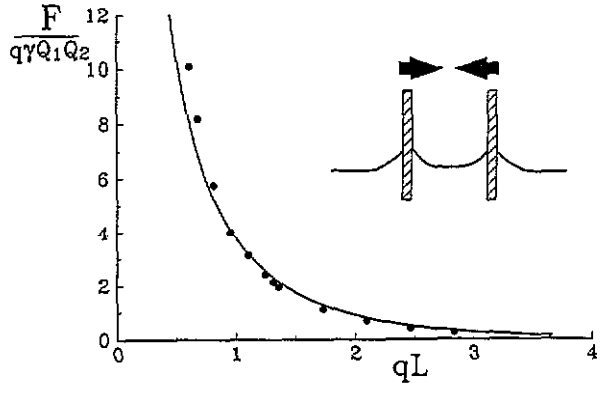

Figure 4. Lateral capillary force, F, versus the distance, L, between two vertical hydrophilic glass capillaries, partially immersed in pure water.

We were able to show that the crystal growth is caused by a convective transport of particles towards the ordered nucleus. This effect appears when menisci (see figure 2(b)) form around the protruding tops of the hydrophilic particles in the nucleus. These menisci hinder the further thinning of the water layer in the nucleus. An intensive water influx from the thicker parts of the layer, which tends to compensate the water evaporation from the nucleus, appears next. This flux carries the suspended particles towards the nucleus. By decreasing or increasing the water evaporation rate we could speed up or slow down the convective particle transport.

3. Theory of the lateral capillary forces

The origin of the lateral capillary forces is the *deformation* of the liquid surface, which is supposed to be flat in the absence of particles. The larger the interfacial deformation created by the particles, the stronger the capillary interaction between them. It is known that two similar particles floating on a liquid interface attract each other [9, 11, 15]—see figure 2(*a*). This attraction appears because the liquid meniscus deforms in such a way that the gravitational potential energy of the two particles decreases when they approach each other. Hence the origin of this force is the *particle weight* (including the Archimedes force).

A force of capillary attraction appears also when the particles (instead of being freely floating) are partially immersed in a liquid layer on a substrate [13, 14]—see figure 2(*b*). The deformation of the liquid surface in this case is related to the *wetting properties* of the particle surface, i.e. to the position of the contact line and the magnitude of the contact angle, rather than to gravity.

To distinguish between the capillary forces in the case of floating particles and in the case of partially immersed particles on a substrate, we call the former lateral *flotation* forces and the latter lateral *immersion* forces. These two kinds of force exhibit similar dependence on the interparticle separation but very different dependences on the particle radius and the surface tension of the liquid. The flotation and immersion forces can be both attractive (figure 2(*a*) and 2(*b*)) and repulsive (figure 2(*c*) and 2(*d*)). This is determined by the signs of the meniscus slope angles ψ_1 and ψ_2 at the two contact lines: the capillary force is attractive when $\sin\psi_1 \sin\psi_2 > 0$ and repulsive when $\sin\psi_1 \sin\psi_2 < 0$. In the case of flotation forces $\psi > 0$ for *light* particles (including bubbles) and $\psi < 0$ for *heavy* particles. In the case of immersion forces between particles protruding from an aqueous layer $\psi > 0$ for *hydrophilic particles* and $\psi < 0$ for *hydrophobic* particles. When $\psi = 0$ there is no meniscus deformation and, hence, there is no capillary interaction between the particles. This can happen when the weight of the particles is too small to create significant surface deformation. The theory [11, 14–16] provides the following expression for calculating the lateral capillary force between two particles of radii R_1 and R_2 separated by a centre-to-centre distance L

$$F = 2\pi\gamma Q_1 Q_2 q K_1(qL)[1 + O(q^2 R_k^2)] \qquad r_k \ll L \tag{1}$$

where γ is the liquid-fluid interfacial tension, r_1 and r_2 are the radii of the two contact lines and $Q_k = r_k \sin\psi_k$ ($k = 1\,2$) is the 'capillary charge' of the particle [15, 19];

$$\begin{aligned} q^2 &= \Delta\rho g/\gamma \qquad &&\text{(in thick films)} \\ q^2 &= (\Delta\rho g - \Pi')/\gamma \qquad &&\text{(in thin films).} \end{aligned} \tag{2}$$

Here $\Delta\rho$ is the difference between the mass densities of the two fluids and Π' is the derivative of the disjoining pressure with respect to the film thickness; K_1 is the modified Bessel function. The asymptotic form of equation (1) for $qL \ll 1 (q^{-1} = 2.7$ mm for water),

$$F = 2\pi\gamma Q_1 Q_2/L \qquad r_k \ll L \ll q^{-1} \tag{3}$$

looks like a two-dimensional analogue of Coulomb's law, which explains the name 'capillary charge' of Q_1 or Q_2. Note that the immersion and flotation forces exhibit the same

functional dependence on the interparticle distance (see equations (1) and (3)). On the other hand, their different physical origin results in different magnitudes of the 'capillary charges' of these two kinds of capillary force. In this aspect they resemble the electrostatic and gravitational forces, which obey the same power law, but differ in the physical meaning and magnitude of the force constants (charges, masses). In the particular case when $R_1 = R_2 = R$; $r_k \ll L \ll q^{-1}$ one can derive [15]

$$\begin{aligned} F &\propto (R^6/\gamma)K_1(qL) \qquad \text{for flotation force} \\ F &\propto \gamma R^2 K_1(qL) \qquad \text{for immersion force.} \end{aligned} \tag{4}$$

Hence, the flotation force decreases, while the immersion force increases, when the interfacial tension γ increases. Besides, the flotation force decreases much more strongly with the decrease of R than the immersion force. Thus $F_{\text{flotation}}$ is negligible for $R < 10\ \mu$m, whereas $F_{\text{immersion}}$ can be significant even when $R = 10$nm. This is demonstrated in figure 3 where the two types of capillary interaction are compared for a wide range of particle sizes. The values of the parameters used are particle mass density $\rho_p = 1.05\ \text{gcm}^{-3}$, surface tension $\gamma = 72\ \text{mNm}^{-1}$, contact angle $\alpha = 30°$, interparticle distance $L = 2R$, and thickness of the non-disturbed planar film $l_0 = R$. The drastic difference between the two types of capillary force is due to the different deformation of the water–air interface, which in turn is determined by the force exerted on the three-phase contact line. The small floating particles are too light to create substantial deformation of the liquid surface. In the case of immersion forces the particles are restricted in the vertical direction by the solid substrate. Therefore, as the film becomes thinner, the liquid surface deformation increases, thus giving rise to a strong interparticle attraction. Hence, the immersion forces may be one of the main factors causing the observed self-assembly of small colloidal particles [5, 6] and protein macromolecules [1, 2, 4] confined in thin liquid films or lipid bilayers.

4. Direct measurements of lateral capillary forces

4.1. Immersion force between two vertical cylinders

A special type of balance was designed and used [18] for measurement of the capillary forces between two vertical cylinders (capillaries)—see the inset in figure 4. Menisci are formed around the cylinders, which leads to the appearance of a lateral capillary force between them. One cylinder is connected to a balance, which measures the horizontal component of the force acting on it. A precise piezoresistive sensor, originally designed as a sensitive pressure transducer (163 PC 01D, Microswitch Inc., USA), is used to convert the force to an electric signal. The precision of the balance is better than 3×10^{-7} N.

Figure 4 presents the dimensionless capillary force $F/(q\gamma Q_1 Q_2)$ between two hydrophilic glass cylinders of radii $r_1 = 370\ \mu$m and $r_2 = 315\ \mu$m as a function of the dimensionless distance qL. The liquid phase is pure water with surface tension $\gamma = 72.4 \pm 0.5\ \text{mN m}^{-1}$, which corresponds to a capillary length $q^{-1} = 2.72$ mm. The experimental data are averaged over three independent runs and are presented by the solid circles. The reproducibility and accuracy of the data are indicated by the size of the circles. The force corresponds to attraction between the two cylinders and slowly decays with the interparticle distance. The magnitude of the force is $F = 1.25 \times 10^{-5}$ N at $qL \simeq 1$. The solid curve in figure 4 presents the result predicted by equation (1). One sees that at large distances ($qL \geqslant 1$) the experimental data are very well represented by the theoretical expression. At smaller separations equation (1) underestimates the force.

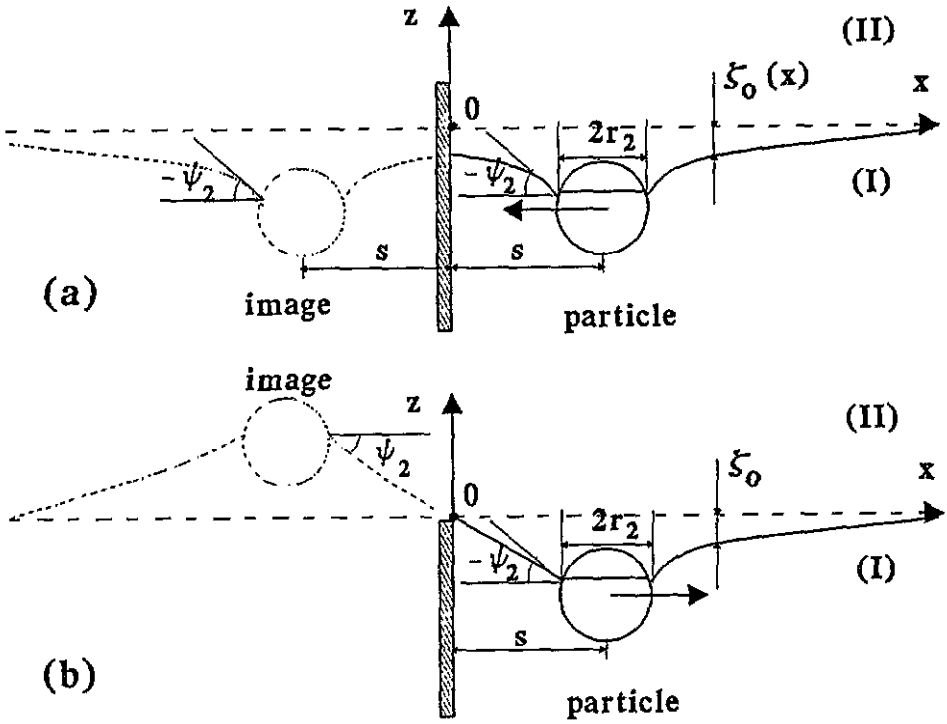

Figure 5. Configurations corresponding to attractive (*a*) and repulsive (*b*) capillary image forces between a floating particle and a wall.

4.2. Capillary image forces

Imagine a floating spherical particle in the vicinity of a vertical planar wall. Below we will use indices 1 and 2 to denote properties belonging to the wall and particle, respectively. We consider the simpler case, when the contact angle at the wall is $\alpha_1 = \pi/2$; hence $\psi_1 = \pi/2 - \alpha_1 = 0$. (The more general configuration with $\psi_1 \neq 0$ is considered in [19].) In this case the meniscus would be flat ($\zeta \equiv 0$) if the floating particle were removed. We denote by $\zeta_0(x, y)$ the meniscus shape in the presence of the particle. Since $\psi_1 = 0$ the function $\zeta_0(x, y)$ must satisfy the boundary condition $(\partial\zeta_0/\partial x)|_{x=0} = 0$ at the wall surface. By using considerations for symmetry one can realise [19] that the function $\zeta_0(x, y)$ would be the same if (instead of a wall at a distance s from the particle) one has a second particle (*image*) floating at a distance $2s$ from the original one—see figure 5(*a*). The 'image' must be identical to the original particle with respect to the size, weight and contact angle. In other words, the spherical particle and its image ought to have identical 'capillary charges', Q_2. For two identical floating particles the lateral capillary force is always attractive [11, 15]. Hence, the particle and its image, depicted in figure 5(*a*), will attract each other, i.e. in reality the wall will attract the floating particle. Moreover, the resulting image force will obey equation (1) with $Q_1 = Q_2$.

The alternative boundary condition $\zeta_0|_{x=0} = 0$ represents a requirement for a zero elevation of the contact line at the wall. This can be realized in practice if the contact line is attached to the edge of a vertical plate, as shown in figure 5(b), or to the boundary between a hydrophilic and hydrophobic domains on the surface of the wall. By using again considerations for symmetry, one can realise that the function $\zeta_0(x, y)$ would be the same

if (instead of a wall at a distance s from the particle) one has a second particle (image) of the *opposite* capillary charge ($Q_1 = -Q_2$) at a distance $2s$ from the original particle. In such a case the lateral capillary force is repulsive, i.e. in reality the wall will repel the floating particle.

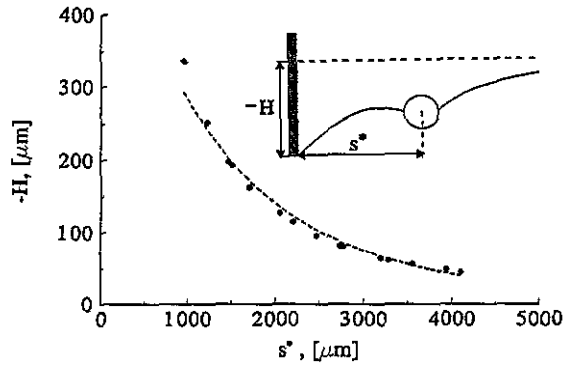

Figure 6. Meniscus lowering at the plate edge, H, versus the equilibrium particle–wall separation, s^*, for a floating copper sphere with hydrophobized surface.

The theory of the capillary image forces was verified [20] by using the vertical plate method, sketched in the inset in figure 6. For each given depth of immersion, H, of the lower edge of a hydrophobic plate (figure 6) the floating particle rests in an equilibrium position at some distance s^* from the wall. In this position the capillary image force, repelling the particle from the wall, is exactly counterbalanced by the gravitational force (including the upthrust).

In figure 6 the experimental results (the circles) for a copper bead are shown. The respective theoretical curve calculated with contact angle $\alpha_2 = 100°$ and particle radius $R_2 = 711$ μm is also plotted [19]. The radius of the same particle, measured by optical microscopy, is $R_2 = 700 \pm 15$ μm. The experimental data show that the larger in magnitude H (i.e. the larger the surface deformation created by the wall), the smaller is the equilibrium separation. The accuracy and reproducibility of the measurements are about ± 2 μm for H and ± 20 μm for s^*. As seen from figure 6 the agreement between the theoretical curve and the experimental points is very good.

References

[1] Yoshimura H, Matsumoto M, Endo S and Nagayama K 1990 *Ultramicroscopy* **32** 265
[2] Nagayama K 1992 *Nanobiology* **1** 25
[3] Hayashi S, Kumamoto Y, Suzuki T and Hirai T 1991 *J. Colloid Interface Sci.* **144** 538
[4] Harris J R, Ceika Z, Wegener-Strake A, Gebauer W and Markl J 1992 *Micron Microsc. Acta* **23** 287
[5] Denkov N D, Velev O D, Kralchevsky P A, Ivanov I B, Yoshimura H and Nagayama K 1993 *Nature* **361** 26
[6] Denkov N D, Velev O D, Kralchevsky P A, Ivanov I B, Yoshimura H and Nagayama K 1992 *Langmuir* **8** 3183
[7] Hinsch K 1983 *J. Colloid Interface Sci.* **92** 243
[8] Camoin C, Roussel J F, Faure R and Blanc R 1987 *Europhys. Lett.* **3** 449
[9] Nicolson M M 1949 *Proc. Camb. Phil. Soc.* **45** 288
[10] Gifford W A and Scriven L E 1971 *Chem. Eng. Sci.* **26** 287

[11] Chan D Y C, Henry J D and White L R 1981 *J. Colloid Interface Sci.* **79** 410
[12] Fortes M A 1982 *Can. J. Chem.* **60** 2889
[13] Kralchevsky P A, Paunov V N, Ivanov I B and Nagayama K 1992 *J. Colloid Interface Sci.* **151** 79
[14] Kralchevsky P A, Paunov V N, Denkov N D, Ivanov I B and Nagayama K 1993 *J. Colloid Interface Sci.* **155** 420
[15] Paunov V N, Kralchevsky P A, Denkov N D and Nagayama K 1993 *J. Colloid Interface Sci.* **157** 100
[16] Kralchevsky P A and Nagayama K 1993 *Langmuir* at press
[17] Paunov V N, Kralchevsky P A, Denkov N D, Ivanov I B and Nagayama K 1992 *Colloids Surf.* **67** 119
[18] Velev O D, Denkov N D, Paunov V N, Kralchevsky P A and Nagayama K 1993 *Langmuir* **9** 3702
[19] Kralchevsky P A, Paunov V N, Denkov N D and Nagayama K 1993 *J. Colloid Interface Sci.* submitted
[20] Velev O D, Denkov N D, Paunov V N, Kralchevsky P A and Nagayama K 1993 *J. Colloid Interface Sci.* submitted